Journal of the Korean Nuclear Society
Volume 32, Number 2, pp.169~179, April 2000

Numerical Analysis of Evolution of Thermal Stratification in a Curved Piping System

Seok Ki Choi and Ho Yun Nam
Korea Atomic Energy Research Institute
150 Dukjin-dong Yusong-gu, Taejon 305-353, Korea
skchoi@kaeri.re.kr

Jong Chull Jo
Korea Institute of Nuclear Safety
19 Kusung-dong, Yusong-gu, Taejon, 305-338, Korea

(Received October 7, 1999)

Abstract

A detailed numerical analysis of the evolution of thermal stratification in a curved piping system in a nuclear power plant is performed. A finite volume based thermal-hydraulic computer code has been developed employing a body-fitted, non-orthogonal curvilinear coordinate for this purpose. The cell-centered, non-staggered grid arrangement is adopted and the resulting checkerboard pressure oscillation is prevented by the application of momentum interpolation method. The SIMPLE algorithm is employed for the pressure and velocity coupling, and the convection terms are approximated by a higher-order bounded scheme. The thermal-hydraulic computer code developed in the present study has been applied to the analysis of thermal stratification in a curved duct and some of the predicted results are compared with the available experimenta data. It is shown that the predicted results agree fairly well with the experimental measurements and the transient formation of thermal stratification in a curved duct is also well predicted.

Key Words : finite volume method, non-orthogonal curvilinear coordinate, momentum interpolation method, SIMPLE algorithm,thermal stratification

1. Introduction

Some safety-related piping systems connected to reactor coolant systems at operating nuclear power plants are known to be potentially susceptible to unanticipated flow-induced thermal stratification which can lead to thermal fatigue damage to the piping systems. Several plants have so far experienced such serious mechanical damages due to thermal fatigue such as pressurizer surge line movements and its support failures, and cracks in feedwater nozzle, high pressure safety

injection lines, and residual heat removal lines. Thus, the USNRC (United States Nuclear Regulatory Commission) has provided generic communications [1-4] to its licensees addressing safety issues arising from thermal stresses and fatigue caused by thermal stratification.

The temperature difference in the fluid region due to the thermal stratification produces thermal stress in the pipe both in axial and circumferential directions. Several investigators have made efforts to determine the temperature distributions in the pipe wall by means of laboratory testing of particular geometry, field measurement of temperature or fully theoretical predictions. Talja and Hansjosten [5] and Wolf et al. [6] have made experimental efforts to measure the temperature distributions in a horizontal pipe wall and compared the measured and calculated stresses due to the thermal stratification phenomena. Basic theoretical predictions either by analytical method [7] or numerical method [8,9] have also been performed to understand the basic features of thermal stratification phenomena. Some investigators have made practical turbulent calculations for analyzing the thermal stratification in the surge line of PWR (pressurized water reactor). Abou and Barois [10] have performed steady, two-dimensional calculations for predictions of stratified pipe flows in PWR. The calculated fluid temperatures have been compared with measured values. Baron et al. [11] have made three-dimensional, unsteady turbulent calculations for recirculating and stratified pipe flow in PWR using the k-ϵ turbulence model and curvilinear coordinates. They compared their results with experimental measurements and reasonably good agreements are observed. Some transient features of thermal stratification in a curved pipe are also investigated. Recently, Baik et al. [12] have carried out unsteady, three-dimensional calculations for analyzing thermal stratification in the surge line of the Korean next generation reactor using the commercial code. The surge line was modeled by a straight pipe line slightly curved at both ends. A parametric study has been carried out to investigate the effect of inlet velocity, temperature difference and pipe slope on the development of thermal stratification. However, their study is not detailed enough to fully understand the development of thermal stratification in piping systems and their results were not validated through comparison with experimental data.

The piping systems in a nuclear power plant have complicated shaped boundaries, which require the use of non-orthogonal curvilinear coordinates for the numerical solution of fluid flow and heat transfer inside the piping system. The present state of the art of computational fluid dynamics can provide numerical solutions for these problems without difficulties. To the author's present knowledge there does not exist a detailed measurement that clearly shows the evolution of thermal stratification in the piping systems. Ushijima [13] has provided some experimental measurements which show the transient evolutions of temperature field in a curved duct. Ushijima [13] has also carried out numerical calculations for velocity distributions, secondary flow patterns and temperature profiles for the evolution of thermal stratification in a curved duct.

In the present study, a three-dimensional thermal-hydraulic computer code for analyzing the thermally stratified flows in a curved piping system has been developed by using body-fitted, non-orthogonal curvilinear coordinates. The cell-centered, non-staggered grid arrangement is adopted and the resulting checkerboard pressure oscillation is prevented by the application of momentum interpolation method [14]. The SIMPLE algorithm [15] is employed for the

pressure and velocity coupling. The convection term is approximated by a higher-order bounded convection scheme. The transient behaviors of stratified fluid flow in a curved duct are simulated and the predicted results are compared with available experimental measurements. The main emphasis of present study is made on the detailed investigation of the transient evolution of thermal stratification such as temperature and velocity fields in a curved duct.

2. Mathematical Formulation

2.1. Governing Equations

For simplicity, it is assumed the thermally stratified fluids are Newtonian with constant properties and the Boussinesq approximation is valid. Then the governing equations for conservation of mass, momentum and energy in a generalized coordinate system x^j can be written as follows [16]:

$$\frac{\partial}{\partial x^j}(U_j)=0$$

$$\frac{\partial}{\partial t}(J\rho u_i)+\frac{\partial}{\partial x^j}\left[U_j u_i-\frac{\mu}{J}\left\{\frac{\partial u_i}{\partial x^m}B_m^j+b_k^j w_i^k\right\}+Pb_i^j\right] \quad (1)$$

$$=\rho g_i\beta(T-T_{ref})J \quad (2)$$

$$\frac{\partial}{\partial t}(J\rho c_p T)+\frac{\partial}{\partial x^j}\left[U_j c_p T-\frac{k}{J}\frac{\partial T}{\partial x^m}B_m^j\right]=0 \quad (3)$$

where

$$U_i=\rho u_k b_k^i,\quad B_m^j=b_k^j b_k^m,\quad w_j^i=\frac{\partial u_i}{\partial x^k}b_j^k \quad (4)$$

and u_i denotes one of the three Cartesian velocity components in the directions of the transformed coordinates $y^i = y^i(x^j)$, the geometric coefficients b_i^j represent the cofactors of $\partial y^i/\partial x^j$ in the Jacobian matrix of the coordinate transformation, J stands for the determinant of the Jacobian matrix and y^i is the Cartesian coordinate system. In the above equations, ρ, μ, p, k, c_p, β, g and T denote respectively density, viscosity, pressure, thermal, thermal conductivity, specific heat, volumetric coefficient of thermal expansion, gravitational acceleration and temperature. In addition, T_{ref} is the reference temperature.

2.2. Initial and Boundary Conditions

Consider a general situation of thermally stratified flow in a curved duct where a fluid of high temperature is flowing through the duct at a constant flow rate so that the steady flow condition is maintained, and then the inlet temperature is lowered at a certain point of time. As the solution domain is symmetric geometrically, only half of the solution domain is solved. Thus, at the symmetry plane, the symmetry boundary conditions are applied for both velocity components and temperature. On the solid wall, no slip and adiabatic boundary conditions are specified. For this situation the boundary conditions are given by

$$u_i=u_{i,in},\quad T=T_{in}$$
: at the inlet of the duct, (5a)

$$u_i=0,\quad \left.\frac{\partial T}{\partial n}\right|_{x^2}=\left.\frac{\partial T}{\partial n}\right|_{x^3}=0$$
: at the inner surface of the duct, (5b)

$$u_2=0,\quad \frac{\partial u_1}{\partial x^2}=\frac{\partial u_3}{\partial x^2}=0,\quad \frac{\partial T}{\partial x^2}=0$$
: at the symmetry plane, (5c)

$$\frac{\partial T}{\partial x^1}=0$$
: at the outlet of the duct. (5d)

At the outlet, the velocity components are

adjusted to satisfy the overall mass conservation.

2.3. Discretization of Governing Equations

The solution domain is divided into a finite number of hexahedral control volume cells. A typical control volume is shown in Fig.1. The discretization of the governing equations is performed following the finite volume approach The convection terms are approximated by a higher-order bounded scheme COPLA developed by Choi et al. [17] and the unsteady term is treated implicitly using the three-level second order scheme suggested by Ferziger and Peric [18].

2.4. Momentum Interpolation Method

In the present study, the Rhie and Chows scheme [14] is modified to obtain a converged solution for unsteady flows which is independent of the size of time step and relaxation factors. The momentum equations are solved implicitly at the cell-centered locations in the Rhie and Chows scheme. The discretized form of momentum equations for the cell-centered velocity components can be written as follows with the under-relaxation factors expressed explicitly;

$$u_{1,p} = (H_{u_1})_p + (D^1_{u_1})_p (P_w - P_e) + (D^2_{u_1})_p (P_s - P_n)_p \quad (6)$$
$$+ (D^3_{u_1})_p (P_b - P_t)_p + (E_{u_1})_p \frac{(4u^{n-1}_{1,p} - u^{n-2}_{1,p})}{2} + (1-\alpha_{u_1}) u^{l-1}_{1,p}$$

where
$$H_{u_1} = \alpha_{u_1} \left\{ \sum A^{u_1}_{nb} u_{1,nb} + (S^{u_1}_c \Delta V) \right\} / A^{u_1}_p \quad (7a)$$
$$D^j_{u_1} = \alpha_{u_1} b^j_i / A^{u_1}_p \quad (7b)$$
$$E_{u_1} = \frac{\alpha_{u_1} \rho \Delta V}{\Delta t} \Big/ A^{u_1}_p \quad (7c)$$
$$A^{u_1}_p = \sum A^{u_1}_{nb} - S^{u_1}_p \Delta V + \frac{3\rho \Delta V}{2\Delta t} \quad (7d)$$

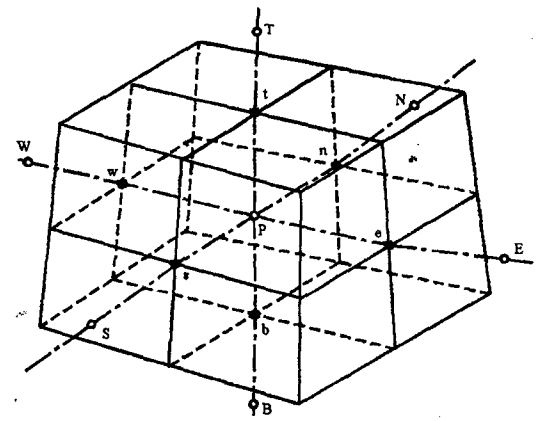

Fig.1. A typical Control Volume

and α_{u_i} are the under-relaxation factors for u_i velocity components and the superscripts n-1, n-2, l-1 denote the previous time steps and iteration level, respectively. The discretized form of momentum equations for the cell-face velocity component, for example u_i at the east face, can be written as follows;

$$u_{1,e} = (H_{u_1})_e + (D^1_{u_1})_e (P_p - P_E) + (D^2_{u_1})_e (P_{se} - P_{ne})$$
$$+ (D^3_{u_1})_e (P_{be} - P_{te}) + (E_{u_1})_e \frac{(4u^{n-1}_{1,e} - u^{n-2}_{1,e})}{2} \quad (8)$$
$$+ (1-\alpha_{u_1}) u^{l-1}_{1,e}$$

In the present modified Rhie and Chows scheme, this cell-face (the east face) velocity component is obtained explicitly through the interpolation of momentum equations for the neighboring cell-centered Cartesian velocity components. The following assumptions are introduced to evaluate this cell-face velocity component.

$$(H_{u_1})_e \approx f^+_e (H_{u_1})_E + (1-f^+_e)(H_{u_1})_p \quad (9a)$$

$$(D^2_{u_1})_e (P_{se} - P_{ne}) \approx f^+_e (D^2_{u_1})_E (P_s - P_n)_E + (1-f^+_e)(D^2_{u_1})_p (P_s - P_n)_p \quad (9b)$$

$$(D^3_{u_1})_e (P_{be} - P_{te}) \approx f^+_e (D^3_{u_1})_E (P_b - P_t)_E + (1-f^+_e)(D^3_{u_1})_p (P_b - P_t)_p \quad (9c)$$

$$\frac{1}{(A_p^{u_i})_e} \approx \frac{f_e^+}{(A_p^{u_i})_E} + \frac{(1-f_e^+)}{(A_p^{u_i})_p} \tag{9d}$$

where f^+_e is the geometric interpolation factor defined in terms of distances between nodal points. Similar assumptions can be introduced for evaluating the velocity components at the north and top faces. Using the above assumptions, the velocity component $u_{i,e}$ can be obtained as follows;

$$\begin{aligned} u_{1,e} &= \left[f_e^+ u_{1,E} + (1-f_e^+)u_{1,p} + (D^1_{u_1})_e (P_p - P_E)\right. \\ &\quad \left. - f_e^+ (D^1_{u_1})_E (P_w - P_e)_E - (1-f_e^+)(D^1_{u_1})_p (P_w - P_e)_p\right] \\ &\quad + (1-\alpha_{u_1})\left[u^{l-1}_{1,e} - f_e^+ u^{l-1}_{1,E} - (1-f_e^+)u^{l-1}_{1,p}\right] \\ &\quad + \frac{\alpha_{u_1}\rho}{\Delta t}\left[\frac{(\Delta V)_e}{(A_p^{u_1})_e}\frac{(4u^{n-1}_{1,e} - u^{n-2}_{1,e})}{2} - f_e^+\frac{(\Delta V)_E}{(A_p^{u_1})_E}\frac{(4u^{n-1}_{1,E} - u^{n-2}_{1,E})}{2}\right. \\ &\quad \left. - (1-f_e^+)\frac{(\Delta V)_p}{(A_p^{u_1})_p}\frac{(4u^{n-1}_{1,p} - u^{n-2}_{1,p})}{2}\right] \end{aligned} \tag{10}$$

The term in the first bracket of the right hand side of Eq. (10) is the original Rhie and Chows scheme [14]. Majumdar [19] has revealed that omission of the term in the second bracket leads to a converged solution which is relaxation factor dependent. Recently, Choi [20] added the term in the last bracket to obtain the converged solution that is independent of the size of time step and relaxation factors for unsteady flow calculations. The SIMPLE algorithm [15] is used for pressure-velocity coupling and the details of use of this algorithm with the momentum interpolation method are well documented in Peric [16] and are not reproduced here.

3. Results and Discussion

The numerical solution method presented in the present study is applied to the analysis of thermal stratification in a curved duct, as shown in Fig.2, experimentally studied by Ushijima [13].

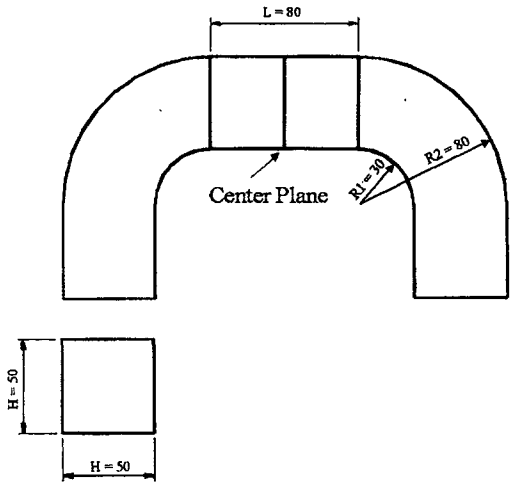

Fig. 2. Geometry of Curved Duct

Calculations are performed for the symmetric half of the duct. The $74 \times 22 \times 42$ numerical grids are generated algebraically. The Reynolds number based on the hydraulic diameter of the duct and the inlet velocity is 500, and the Richardson number is 9.8. Since the Richardson number is relatively high, the buoyancy force affects strongly the flow field. First, the steady state solution is obtained with the temperature maintained at high temperature and then the transient solutions are obtained using the steady state solution as an initial condition. The inlet temperature is assumed to be lowered linearly 10 degrees during the initial 30 seconds, which approximately simulates the experimental condition. Calculations are continued until 120 seconds using the time step size of 0.1 second. The convergence is declared at each time step when the maximum of the absolute sum of the dimensionless residuals of momentum equations, pressure correction equation and energy equation is less than 10^{-4}.

Fig. 3 shows the transient evolution of temperature field at the symmetry plane. The predicted temperatures are normalized using the hot and cold temperatures, and the interval of the isothermal line is 0.1. It is noted that the duct is

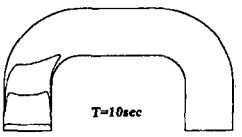

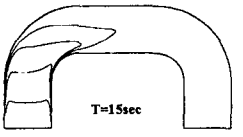

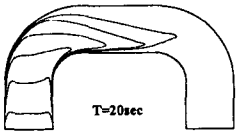

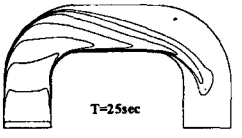

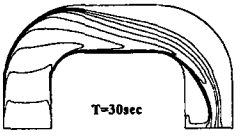

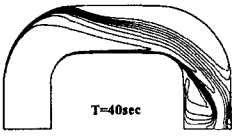

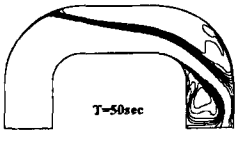

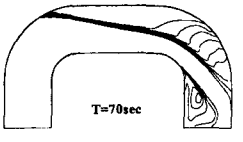

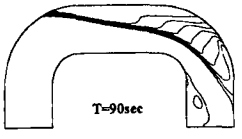

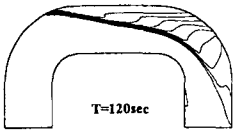

Fig. 3. Development of Temperature Field at the Symmetry Plane

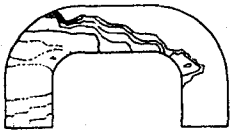
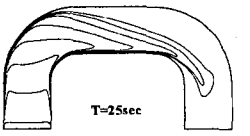

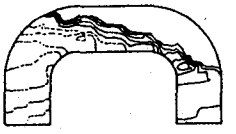
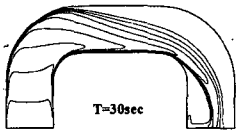

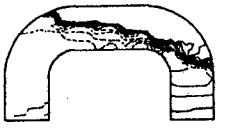
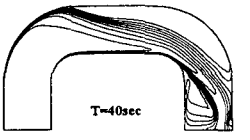

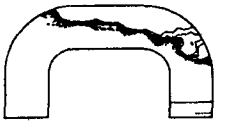
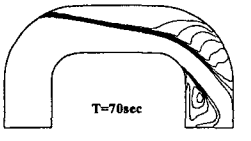

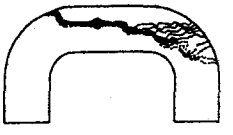
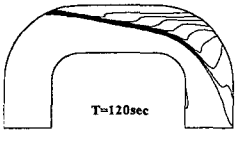

Fig. 4. Comparison Between Experiments and Calculated Results for Temperature Field (left: experimental results, right: calculated results)

filled with hot fluid initially and the inlet temperature is lowered linearly during the initial 30 seconds. At the initial stage (t=10sec) the inlet cold fluid moves upward pushing the hot fluid in the downstream direction. When the cold fluid reaches the first curved section (t=15sec), it begins to flow into the lower side of the duct with the force balanced between inertia of the inlet flow and buoyancy of the hot fluid. Even as the cold fluid moves further downstream (t=20sec) and reaches the outlet (t=30sec), the temperature of fluid in the upper portion of the duct does not change and a mild temperature gradient is established at the interface between hot and cold fluid regions. The temperature gradient at the interface becomes steeper as time elapses and there exists a strong mixing near the outlet (t=50sec). A stable thermal stratification begins to be established in the upper portion of the duct (t=70-90sec), and then the mixing near the outlet is nearly finished and the stable thermal stratification does not change much with time (t=120sec). Since the Richardson number of the present problem is relatively high, the thermally stratified region covers for the upper most portion of the duct. One thing we note here is that the cold fluid can not mix well with the hot fluid once the thermal stratification is established.

Fig.4 shows the comparison of predicted temperature distribution at the symmetry plane

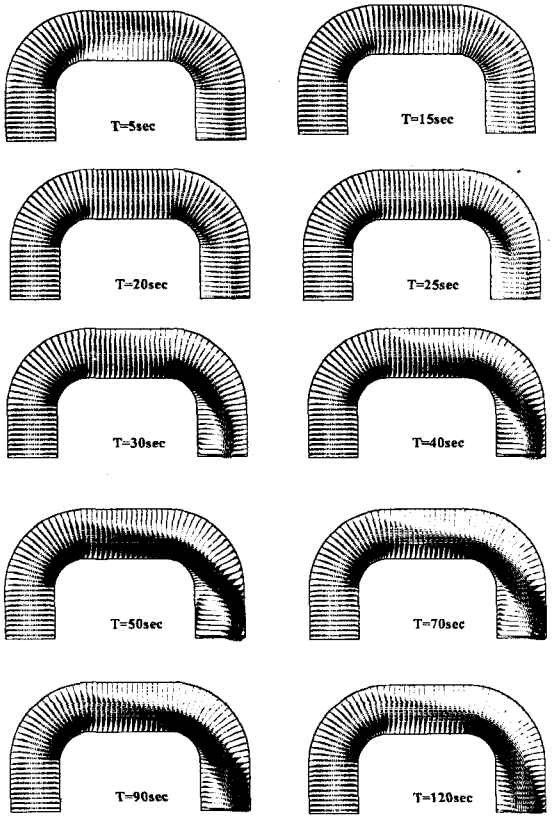

Fig. 5. Development of Velocity Field at the Symmetry Plane

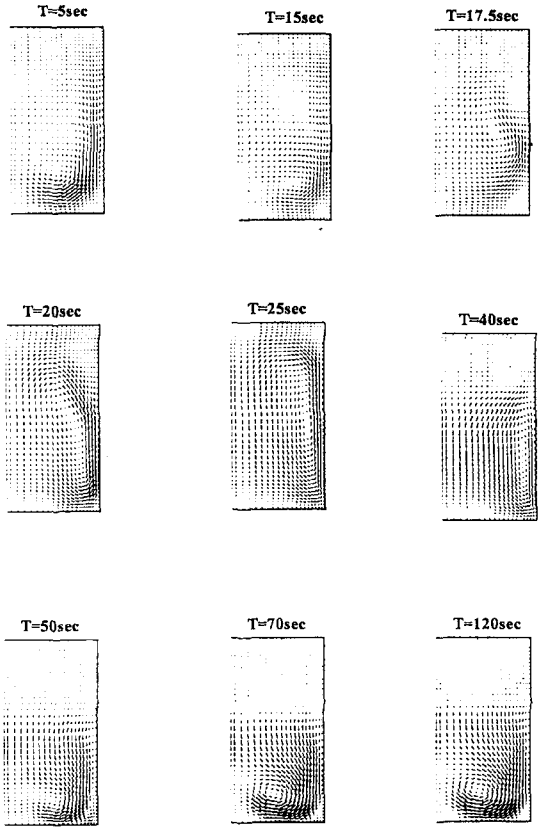

Fig.6. Development of Secondary Motion at the Center Plane

with the measured data by Ushijima [13]. We observe that the numerically predicted results agree fairly well with the experimental measurements, especially when the thermal stratification is established (t=120sec). Some discrepancies may be partly due to the differences in inlet conditions between the measurement and calculation, which can be observed in the initial development of the temperature field in the measured data. The inlet temperature distributions in the measured data during the initial 30 seconds are not varied linearly and are not uniformly distributed. Therefore, it is very difficult to impose a correct inlet condition for calculation that matches with the experimental condition. However, we can notice that a slightly different imposition of inlet temperature in the initial period of time does not much influence the final formation of thermal stratification. It is also noted that the measured data are not smooth due to the use of an insufficient number of thermocouples.

Fig.5 shows the development of velocity field at the symmetry plane. At the initial stage (t=5-15sec) the velocity field is not changed. When the thermal stratification has begun to form balancing the inertia and buoyancy forces, the magnitude of fluid flows near the lower side of duct becomes larger (t=20sec). There is a strong movement of cold fluid when the cold fluid passes the second curved section (t=25-40sec) since the incoming cold fluid could not penetrate into the hot fluid region. The strong movement of cold fluid pushes

the existing hot fluid in both upward and downward directions and it induces a counterclockwise movement of hot fluid in the upper region of the duct and a strong clockwise vortex near the outlet (t=50sec). There exists a strong mixing near the outlet of the duct. As time elapses, the cold fluid flows into the outlet mixing with hot fluid and the counterclockwise vortex in the upper right region of the duct becomes weak (t=70sec). There still exists a mixing near the outlet and the flow in this region is developing while the flow in the upper region of the duct is nearly quiescent (t=90sec). When the mixing process near the outlet is finished, the velocity field in this region as well as the other region is nearly established (t=120sec). We can see that the development of velocity field is consistent with that of the temperature field.

Fig.6 shows the development of a secondary motion at the cross-section of the center plane of the duct. There exists a relatively strong vortex initially (t=5sec) and the magnitude of vortex becomes weak as the mixing process continues (t=15-17.5sec). Then the secondary motion changes rapidly (t=20-50sec) and a complicated evolution of secondary motion continues until a stable stratification is established (t=70sec). After the stable stratification is established, the secondary motion in the hot fluid region is very weak and there exists a strong clockwise vortex at the right-bottom corner of the duct due to the relatively high strength of the primary motion in this region.

Fig.7 shows the predicted isothermal lines at the cross section of the center plane of the duct. These figures show well the development of the thermal stratification. At an earlier stage of the mixing process the temperature gradient near the lower wall is small and a little strange evolution of the temperature field in this region is due to the smearing of cold fluid, which can be seen in Fig.3.

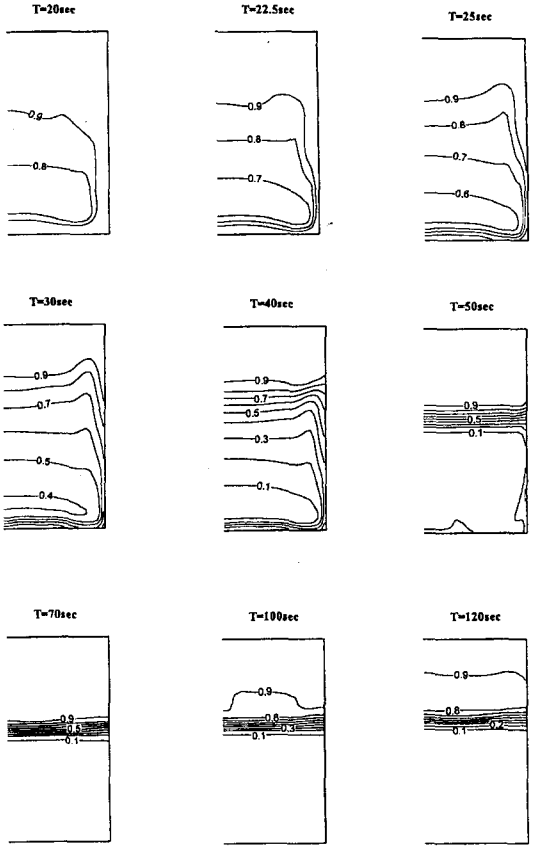

Fig. 7. Development of Temperature Field at the Center Plane

The temperature gradient at the interface between cold fluid and hot fluid becomes steeper as the stratification is established (t=50sec). A steep temperature gradient is established around t=70sec. Then the temperature gradient at the upper portion of the interface becomes smaller (t=100-120sec) due to the heat transfer at the interface of hot and cold fluids.

Fig.8 shows the comparision of calculated results with measured data for vertical temperature distribution at t=120sec for three sections at the symmetry plane (section A : end of first curved section, section B : center plane, section C : start of second curved section). Although the numerically predicted results of thermal interface is

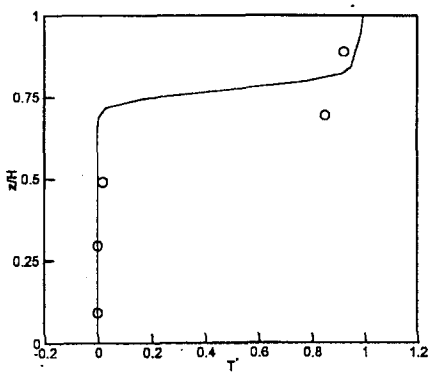

(a) Section A

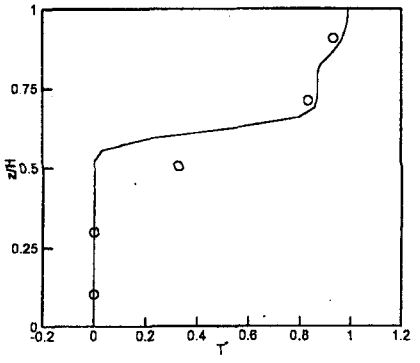

(b) Section B

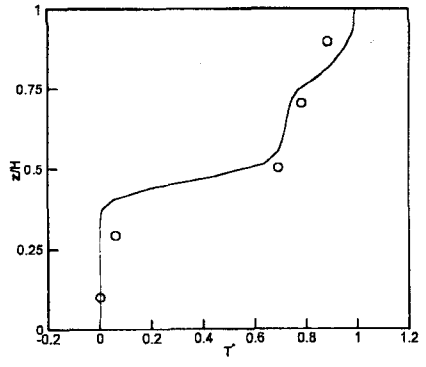

(c) Section C

Fig.8. Vertical Temperature Distributions at Three Sections of the Symmetry Plane

located slightly higher than that of experimental measurements, the present calculation method predicts satisfactorily the vertical temperature distributions. The present predictions agree fairly well with previous predictions by Ushijima [13]. The small discrepancies may be due to the use of different numerical method and numerical grids.

The calculation method presented in the present study predicts well the thermal stratification process in a curved duct. The predicted temperature fields agree well with the experimentally measured results, and the primary motion as well as the evolution of a secondary motion are well predicted. The present calculation method can be applied to the prediction of thermal stratification in various piping systems, especially those in the nuclear power plant.

4. Conclusions

An numerical method for calculating the thermally stratified flows in a curved piping system has been presented. The method employs a body-fitted, non-orthogonal grid system to accommodate the various shapes of a piping system and an advanced convection model to obtain an accurate solution. The use of the momentum interpolation method for unsteady flow in a non-orthogonal grid system is presented. The computer code developed in the present study is applied to the prediction of the thermal stratification in a curved duct and it is shown that the computed results agree well with the experimental measurements. The favorable results obtained from the present computer code show that the present computer code can be applied to the prediction of practical thermal stratification phenomena in a nuclear power plant. The thermal stratification in a practical nuclear power plant involves temperature gradient, oscillations of the stratification interface and inherent local

temperature fluctuations. Time-variations of the temperature due to the turbulent fluctuations can be as critical as the spatial variations. In this case the large eddy simulation method can be an attractive method of predicting instantaneous flow topology, time-dependent turbulent interaction and therefore the temperature fluctuation. Introduction of the large eddy simulation method in the present thermal hydraulic computer code is under way to predict the practical thermal stratification phenomena in a nuclear power plant.

Acknowledgement

This study has been carried out under the Nuclear R&D Program by Ministry of Science and Technology of Korea.

References

1. US NRC Bulletin 79-13, Cracking in Feedwater System Piping, (1979).
2. US NRC Bulletin 88-08, Thermal Stresses in Piping Connected to Reactor Coolant Systems, (1988).
3. US NRC Bulletin 88-11, Pressurizer Surge Line Thermal Stratification, (1988).
4. US NRC NUREG/CR-6456, Review of Industry Efforts to Manage Pressurized Water Reactor Feedwater Nozzle, Piping, and Feedring Cracking and Wall Thinning, (1989).
5. A. Talja and E. Hansjosten, Results of Thermal Stratification Tests in a Horizontal Pipe Line at the HDR- Facility, Nucl. Eng. and Design, vol. 118, pp. 29-41, (1990).
6. L. Wolf, W. Hafner, M. Geiss, E. Hansjosten and G. Katzenmeier, Results of HDR-Experiments for Pipe Loads under Thermally Stratified Flow Conditions, Nucl. Eng. and Design, vol. 137, pp. 387-404, (1992).
7. W. R. Smith, D. S. Cassell and E. P. Schlereth. A Solution for the Temperature Distribution in a Pipe Wall Subjected to Internally Stratified Flow, Proceedings of the 1988 Joint ASME-ANS Nuclear Power Conf., Myrtle Beach, South Carolina, pp. 45-50, (1988).
8. H. K. Youm, M. H. Park and S. N. Kim, The Unsteady 2-D Numerical Analysis in a Horizontal Pipe with Thermal Stratification Phenomena, J. of the Korean Nuclear Society, vol. 28, no. 1, pp. 27-35, (1996).
9. J. C. Jo, Y. I. Kim and S. K. Choi, Heat Transfer Analysis of Thermal Stratification in Piping Connected to Reactor Coolant System, In Proceedings of the 1st Korea-Japan Symposium on Nuclear Thermal Hydraulics and Safety, Paper no. WR-13, pp. 191-198, (1998).
10. Y. Abou-rjeily and G. Barois, Numerical Prediction of Stratified Pipe Flows in PWRs, Nucl. Eng. and Design, vol. 147, pp. 47-51, (1993).
11. F. Baron, M. Gabillard and C. Lacroix, Experimental Study and Three-Dimensional Prediction of Recirculating and Stratified Pipe Flow in PWR, Proceedings of NURETH 4, Karlsruhe, pp. 1354-1361, (1989).
12. S. J. Baik, I. Y. Im and T. S. Ro, Thermal Stratification in the Surge Line of the Korean Next Generation Reactor, Proceedings of OECD NEA/WANO Special Meeting on Experience with Thermal Fatigue in LWR Piping Caused by Mixing and Stratification, Paris, France, (1998).
13. S. Ushijima, Prediction of Thermal Stratification in a Curved Duct with 3D Body-Fitted Co-ordinates, Int. J. for Numerical Methods in Fluids, vol. 19, pp. 647-665, (1994).
14. C. M. Rhie and W. L. Chow, Numerical Study of the Turbulent Flow Past an Airfoil with Trailing Edge Separation, AIAA J., vol. 21,

no. 11, pp. 1525-1532, (1983).

15. S. V. Patankar, Numerical Heat Transfer and Fluid Flow, McGraw-Hill, New York, (1980).
16. M. Peric, A Finite Volume Methods for the Prediction of Three Dimensional Fluid Flow in Complex Ducts, Ph.D. Thesis, Mechanical Engineering Department, Imperial College, London, (1985).
17. S. K. Choi, H. Y. Nam and M. Cho, Evaluation of a Higher-Order Bounded Scheme: Three-Dimensional Numerical Experiments, Numerical Heat Transfer, Part B, vol. 28, pp. 23-38, (1995).
18. J. H. Ferziger and M. Peric, Computational Methods for Fluid Dynamics, Springer Verlag, Berlin Heidelberg, 2nd printing, pp. 134, (1997).
19. M. Majumdar, Role of Under -relaxation in Momentum Interpolation for Calculation of Flow with Non-staggered Grids, Numerical Heat Transfer, vol. 13, pp. 125-132, (1988).
20. S. K. Choi, Note on the Use of Momentum Interpolation Method for Unsteady Flows, Numerical Heat Transfer, Part A, vol. 36, pp. 545-550, (1999).